Thermal systems capabilities using infrared obscurants

G. B. PULPEA[a], I. VEDINAŞ[a], T. ZECHERU[b], E. TRANĂ[a], R. ŞTEFĂNOIU[c], R.M. LUNGU[b], T. ROTARIU[a*]
[a]*Military Technical Academy, 39-49 George Coşbuc, 050141 Bucharest, Romania*
[b]*Scientific Research Center for CBRN Defense and Ecology, 225 Şos. Olteniţei, 041309 Bucharest, Romania*
[c]*University POLITEHNICA of Bucharest, 313 Spl. Independentei, 060042 Bucharest, Romania*

Nowadays, on the battlefield, a clear sight of the target is paramount for a successful engagement. Laser guided rockets and modern sensors that offer new means of targeting and observation have changed modern battle tactics. The equipment evolution has brought optical systems at a new progress peak, which made possible day or night observation in unfavourable conditions. On the reverse side of the observation systems, namely the target (friendly forces) is another factor to be accounted: troops masking. For this aim, new devices, such as pyrotechnic obscurants systems, have been developed to counter modern observation systems, which are in a continuous evolution. Therefore, the first step in optoelectronics systems countering is to study and analyse the way they operate in different regions of the electromagnetic spectrum. In this context, the aim of this paper has been to perform a detailed analysis of the thermal systems regarding their observation capabilities in clear atmosphere and in the presence of infrared obscurants. Using both theoretical and experimental analysis, it has been shown that it is difficult to counter thermal observation systems by pyrotechnic smoke obscurants.

(Received October 3, 2016; accepted February 10, 2017)

Keywords: Thermal sensor, Optoelectronic system, Infrared, Obscurant, Pyrotechnics

1. Introduction and conceptual approach

Night vision systems are based on sensors (the electronic part) designed to enhance or produce an image when the light level is low or it is completely dark. These systems are extremely important for military applications conducted during day or night or in low light conditions. Night vision devices are conceived to increase the visibility level in areas of interest. As observation capabilities, these systems are not able to make "day out of night", but they offer an impressive increase in visibility.

The first devices that appeared in the 60`s were equipped with active sensors that used a supplementary infrared source for image enhancement, but with low performances. Later, due to new developments in the field, passive sensors were developed, like night vision with image enhancers and thermal imaging cameras. Both systems offer impressive performances in various situations and are in the endowment of the modern armies across the world.

Although built to fulfil the same purpose, night vision systems and other optoelectronic devices have completely different functioning principles. Also, system design, target signature, atmospheric effects and obscurant impact on system performance are determined by the different spectral region where each sensor operates (Fig. 1).

Image intensifiers amplify the level of illuminance (residual light) that exists in the visualised scene up to a level to which observing the scene becomes possible by detecting the radiation reflected by the objects in the theatre (Fig. 2).

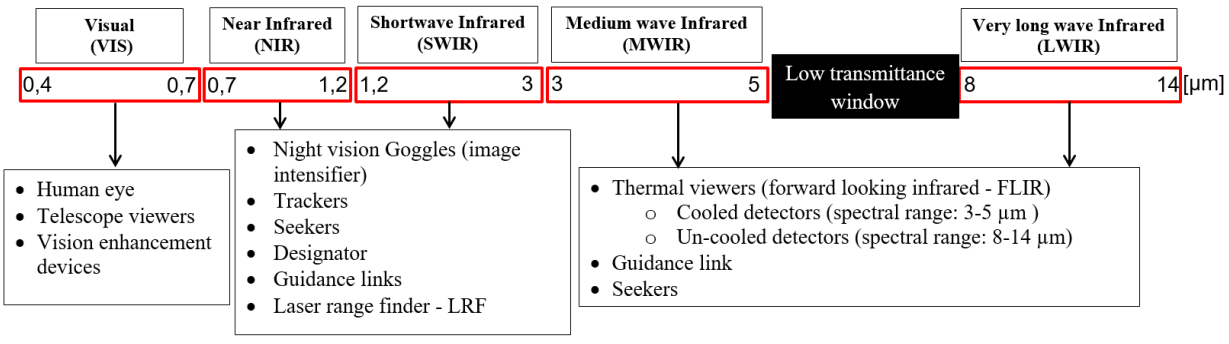

Fig. 1. Sensors spectral regions

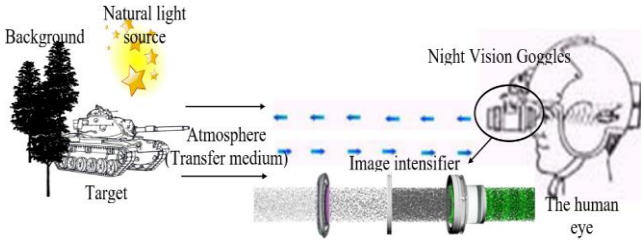

Fig. 2. Operating diagram for passive night vision system

Thermal imaging cameras detect thermal radiation emitted by all existing bodies in the visual field and are based on the thermal contrast between target and background (Fig. 3).

Fig. 3. Thermal energy in everyday life

During day time, in the visible range devices like video cameras or binoculars generate images similar to those of the human eye that use light radiation which are prone to failure due to obscurities in the atmosphere and lack of a light source.

In NIR and SWIR regions, the energy needs to be reflected by the target in order to produce quality images, which means that the existence of an external light source is necessary (radiation from the sun, moon and stars) or an auxiliary source of radiation (LED). An advantage of this technology is that glass allows the passage of radiation with a wavelength below 3 μm [1-3].

MWIR and LWIR regions are often called thermal regions. Devices that operate in these areas can be completely passive. Thermal imaging cameras do not need artificial or natural light sources since this technology is based on radiation emitted by objects. The quality of an image produced by a thermal sensor depends on two factors: the temperature of the object and its emittance. Glass and plastic material are opaque to radiation from LWIR and block entirely the radiation emitted through MWIR [2-3]. Systems that activate in MWIR and LWIR are more tolerant regarding atmospheric obscurants than other optoelectronic systems.

The spectral regions where each sensor can perform are limited by the atmosphere, a propagation medium that limits the system's performance [3]. Natural and artificial obscurants influence the areas of the electromagnetic spectrum where these sensors operate. For a sensor to reproduce an image of the object, the emitted or reflected radiation must be able to pass through the environment from the target to the sensors.

Thermal sensors can be used both during day or night, but the body thermal signature differs significantly, due to daytime solar charging.

The thermal regions differ from the spectrum of the human eye; thus, the thermal image presents significant differences versus a visual image perceived by the human eye. The image produced by a thermal sensor is not stereoscopical and no shadow appears in thermal images shown on a display. Also, writings or details from vehicles or devices are impossible to visualise with thermal cameras.

For the detection of hot objects (such as thermal motors), it is necessary to use the 3-5 μm spectral range. Objects with temperatures around 20 ºC like buildings, vegetation, human body or animals offer a good thermal signature in the 8-14 μm range. This phenomenon is described by the law of Wien presented by the mathematical relations (1)-(3) [1-4],

$$\lambda_{\max} = \frac{b}{T} \tag{1}$$

$$\lambda_b = \frac{b}{T_b} = \frac{2.898 \cdot 10^3 \, \mu m \cdot K}{309.75 \, K} = 9.356 \mu m \tag{2}$$

$$\lambda_t = \frac{b}{T_t} = \frac{2.898 \cdot 10^3 \, \mu m \cdot K}{623.15 \, \mathrm{K}} = 4.651 \mu m \tag{3}$$

where $\lambda_{\max}$ is the maximum of the wavelength, λ_b is thermal radiation of the human body, λ_t is thermal radiation of military technique, T is the absolute temperature of the black body, $T_b = 309.75 \, \mathrm{K}$ is body temperature, $T_t = 350 \, \mathrm{K}$ is tank temperature and b is a constant of proportionality called Wien`s displacement constant, which is equal to $2.898 \cdot 10^3 \, \mu m \cdot K$.

A system is described by its performance and safety characteristics, which fulfil more or less the basic functions of the system. For a thermal vision system the most important and influent parameters in the selection process are defined by spectral region, system resolution and observation distance. *Spectral region* (μm) indicates the usability of the system. *Resolution* (pixels) indicates the minimal size of a target that can be detected and represented on the display module. *Observation distance* (m) represents the distance at which the object can be clearly distinguished from the background (the distance differs according to the size of the targeted object).

Besides these characteristics, the efficiency of using thermal vision systems depends greatly on the quality of the images provided by the optical systems, which increased dramatically within the past years [5-7]. The human observer visualises these images and tries to take decisions about the target (Fig. 4). In the case of thermal cameras, the difference that counts is given only by the training of the observer, his experience achieved by training being decisive.

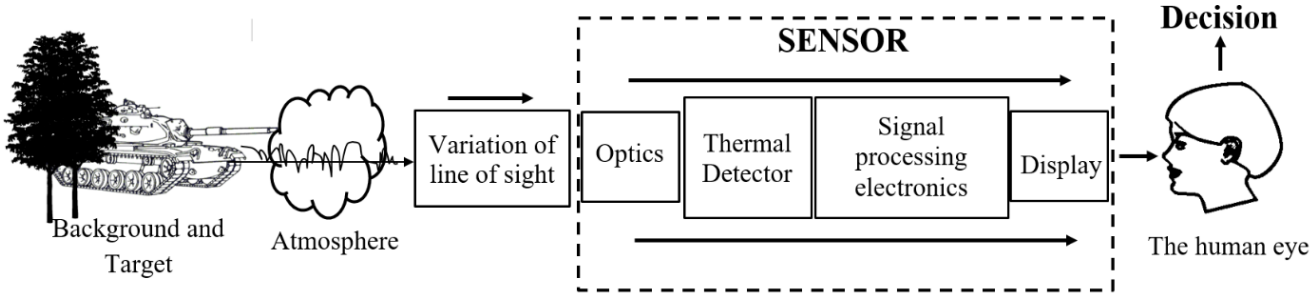

Fig. 4. Target acquisition process components

Thus, for target observation during night or day, the optoelectronic systems needs to fulfil the three steps of observation like detection, recognition and identification that depends on the target distance (Fig. 5). *Detection* implies noticing the target as something different from the background and of importance to the viewer. *Recognition* implies distinguishing the shape of the target and classifying it accordingly. *Identification* is the final step of the process that allows target customization.

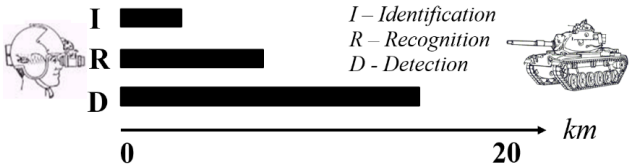

Fig. 5. Optoelectronic system observation distance

The aim of the study was to identify and analyse the optoelectronic systems with high performance in extreme conditions and which are less vulnerable to atmospheric obscurants. By a detailed literature review in the field, a series of characteristics were determined in order to define the thermal system, such as the most performing target acquisition system on the battlefield.

Thermal cameras have observation distances around 10 km [8-9], encounter problems of target identification but are superior regarding the detection and recognition of objects, due to the complexity of the device and the functioning concept. These sensors operate successfully in complete darkness if the target is hot or cold enough versus the background.

An important feature of thermal cameras is the possibility of sighting camouflaged targets. Based on different operating principles, thermal cameras can easily spot small temperature differences between objectives and background.

Rain, snow, and fog reduce the effectiveness of passive systems by reducing atmospheric transmittance. Under bad weather conditions, thermal sensors are affected more versus visible systems by variations in atmospheric water content [10].

The signal radiation from the target that reaches the sensor is reduced by atmosphere passage that can introduce noise in the sensor band, thus decreasing the image quality. The atmospheric parameters used to characterize this signal degradation are atmospheric extinction, transmittance, contrast transmittance and turbulence [10].

Atmospheric extinction represents radiation damping through the atmosphere and can be produced by two processes: absorption and scattering. Its amplitude depends on the type, size and concentration of the atmospheric constituents, but also on the wavelength of the electromagnetic radiation. Gases and water vapour cause significant extinction in the IR bands by absorption [10].

Obscurants are particles suspended in the air (atmosphere) that block or attenuate a part of the electromagnetic spectrum. Besides natural obscurants and those that are created as a result of industrial activity, there were developed military obscurants like pyrotechnic smoke composition designed to counter thermal and sighting sensors. The smoke screen placed between the target and observer is intended to decrease the efficiency of the observation process by their interaction with the emitted radiation of the target.

Natural obscurants create large recognition and identification problems [4, 11] but they can be used in the advantage of the friendly forces only if the weather is accurately predicted. Because of that, artificial obscurants also called infrared obscurants are used to counter enemy optoelectronic systems. The disadvantages of the observation capacities of thermal sensors are amplified if these systems are used against obscurant conditions**.** Placing an obscurant factor in the specified path length basically will conceal threat forces from observation.

Chemical agents generally used in pyrotechnic devices in order to generate smoke curtains for visible and IR screening are mineral oils, metallic fuels with high combustion temperatures (magnesium, aluminium, zinc, titanium), hexachloroethane (HCE) and hexachlorobenzene (HCB) and phosphorus [11-14]. The oil smoke produces effective obscuration in visible through NIR, such as HC smokes, but it is relatively ineffective in MWIR and LWIR [11]. More, HC smoke is carcinogenic and is no longer used in smoke systems [11]. Metallic fuels are usually combined with HC compounds or with polytetrafluoroethylene (PTFE). Phosphorus is a flammable solid that burns in the air to form solid particles of phosphorous pentoxide. The oxide rapidly reacts with atmospheric water (humidity) to generate phosphoric acid through an exothermic reaction. Thus, phosphorus is often

used in instantaneous burst munitions like smoke projectiles, smoke grenades and smoke candles. There are two types of phosphorus used in such applications: white phosphorus (WP) and red phosphorus (RP). WP and RP smokes are effective in visible and NIR and less effective in MWIR and LWIR, but it is still sufficient to defeat thermal systems if used in large quantities [12,14].

Nowadays, due to its high toxicity and pyrophoric nature, WP is less used, while RP becomes the main smoke-generating agent, especially in pyrotechnic compositions where it can be found mixed with powerful oxidizing agents. Moreover, penetration capacity through obscurants like dust, fog, haze or artificial smoke is of interest only in the case of thermal sensors.

2. Theoretical analysis of thermal sensors performances

Further, a theoretical evaluation of the atmosphere and obscurants effects on thermal sensor performance characteristics is made.

The resolution of a thermal system describes the ability of the system to reproduce details in the scene image. Subjective resolution is a performance characteristic that includes the effect of the human observer using the system. This system resolution is translated to field performance using a set of experimental rules known as Johnson criteria and a parameter of probability, the target transfer probability curve. Johnson criteria specify the number of cycles N_{50} (Table 1) that the system must resolve across the target in order to perform a target detection or discrimination task with 50% probability. The levels of performance specified by Johnson criteria are detection, recognition and identification [10].

Table 1. Johnson Criteria N_{50} - 50% probability level [10]

Probability of accomplishing task	Number of cycles resolved across target critical dimension		
	Detection	Recognition	Identification
Thermal sensors	1	4	8

Equations (4)-(8) necessary in order to determine the discrimination probability for a target acquisition (Fig. 6) are described below,

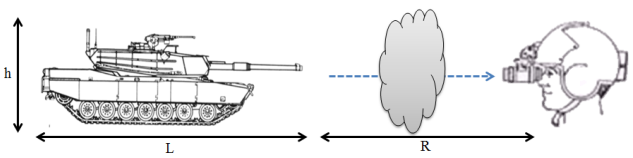

Fig. 6. Target acquisition process

$$d_c = \sqrt{h \cdot L} \tag{4}$$

$$\nu_t = \frac{R}{d_c} \tag{5}$$

$$\Delta T` = T(\lambda) \cdot \Delta T \tag{6}$$

$$N_t = \frac{\nu}{\nu_t} = \frac{d_c \cdot \nu}{R} \tag{7}$$

$$P_O = \frac{N_t}{N_{50}} = \frac{d_c}{R} \cdot \frac{\nu}{N_{50}} = \frac{\sqrt{h \cdot L}}{R} \cdot \frac{\nu}{N_{50}} \tag{8}$$

where d_c *is* target feature size [m], ν_t is target spatial frequency, $\Delta T`$ is the apparent target thermal signature [K], ΔT is target thermal signature [K], N_t *is* number of cycles resolved across the target, N_{50} is number of cycles resolved across target critical dimension (Johnson Criteria N for task accomplishment, 50% probability level), P_O is the observation probability, h is target height [m], L is the target length [m], ν is the spatial frequency [cycles/mrad] and R is the path length [km].

The minimum resolvable temperature (MRT) difference curve, used for a thermal imager, is thus a plot of the bar pattern spatial frequency vs. minimal temperature difference resolvable at that spatial frequency. The subjective resolution curve MRT may be used to determine the system resolution under field conditions. By definition, the MRT curve for a thermal imager gives the minimum resolvable temperature difference required to resolve a bar pattern with spatial frequency [10].

Also, the number of cycles N_t resolved by the system across a specified target is determined from the system MRT curve, the apparent target thermal signature, and the target spatial frequency (size and range to the target).

Besides target and sensor characteristics, the atmospheric transmittance must be described in clear natural atmosphere (precipitation absence) and in screening conditions created by pyrotechnically generated smoke. Transmittance is the quantity that defines the fraction of the original energy left in an electromagnetic beam after its passing along an optical path (R) [10]. The optical path represents a straight line between some initial point (the observer) and the final point (the target). Equations (9)-(16) describe atmosphere transmittance, smoke screens capacity:

$$M_a` = Y_f \cdot M_{gt} \cdot E_f \tag{9}$$

$$M_{sc} = M_g \cdot n \tag{10}$$

$$\rho_s = \frac{M_{gt} \cdot f_s}{L_s \cdot l_s \cdot h_s} \tag{11}$$

$$CL = \rho_s \cdot l_s \tag{12}$$

$$T_s(\lambda) = e^{-\alpha_s(\lambda)\cdot CL} \tag{13}$$

$$T_m(\lambda) = e^{-\gamma_m(\lambda)\cdot R} \tag{14}$$

$$T_a(\lambda) = e^{-\gamma_a(\lambda)\cdot R} \tag{15}$$

$$T(\lambda) = T_m(\lambda)\cdot T_a(\lambda)\cdot T_s(\lambda) \tag{16}$$

where M_a` is the mass of aerosol disseminated [kg], Y_f is the yield factor, E_f is the efficiency factor (0.1-1), M_{sc} is the total mass of smoke composition [kg], M_g is the mass of composition in grenade [kg], n is the number of smoke generators, ρ_s is the aerosol concentration, f_s is the concentration factor (0.1-1), L_s is the dispersal length [m], h_s is the smoke height [m], l_s is the path length of obscurant [m], CL is the concentration path length product [g/m^2], $\alpha_s(\lambda)$ is the mass extinction coefficient, $T_s(\lambda)$ is the smoke transmittance, $T_m(\lambda)$ atmospheric molecular transmittance for water vapours and gaseous absorption, $T_a(\lambda)$ is the atmospheric aerosol transmittance, $T(\lambda)$ is the total atmospheric transmittance, γ_m is the molecular volume extinction coefficient , γ_a is the aerosol volume extinction coefficient and λ is the wavelength [µm] [10].

It must be observed, according to equations (6) and (7), that the value of N_t decreases with the range increase to the target because of changes in the target angular size and apparent signature. The target angular size becomes smaller with target spatial frequency increase. The atmospheric attenuation of the target signature is greater at longer ranges, which reduces the apparent target signature, and consequently reducing the spatial frequency ν .

The purpose of this analysis has been to determine the probability values between 0 and 1 of target observation for thermal sensor, in natural atmosphere (where $T_s(\lambda)=1$) and in atmosphere with pyrotechnic smoke for MWIR (3-5 µm) and LWIR (8-12 µm) region. The analysis result is a graph that shows the curve of discrimination probability based on the path length. To accomplish this task, the equations have been solved using an implemented algorithm in Mathcad® software and considering representative conditions: target (tank *h=2.5 m, L=4.86 m, ΔT=3.5 K*); atmosphere (clear summer afternoon, 50% humidity, 30 ºC, visibility 15 km); obscurant (RP smoke *M_g=0.160 kg, n=24, L_s=36 m, h_s=12 m, l_s=10 m, CL=7.69 g/cm^2*) [10].

The assignment of a qualitative meaning to the numerical quantity is subjectively based upon visual comparison of hundreds of plots [10].

0.80 – 1.00 – Excellent	0.20 – 0.39 Poor
0.55 – 0.79 – Good	0.00 – 0.19 Bad
0.40 – 0.54 - Fair	< Very bad

Based on the results presented in the graphs from Figs. 7-10, it has been demonstrated theoretically that thermal systems performances based on observation distance through natural atmosphere are in agreement with the literature references [8-9,15]. Also here stands out the spectral region 8-12 µm, where atmospheric attenuation of the target signature is more affected. Hence the conclusion that thermal system operating in the 3-5 µm (cooled detector) can provide better quality images in the natural atmospheric condition, a fact already known.

Reported only to the obscurant conditions used in this analysis, the screening smoke reduces a big part of signal radiation reaching a sensor from the target, but does not block it entirely. By this theoretical values, it can be concluded that a thermal system at less than 500 m from the target can provide a qualitative image (0.8-1 probability - excellent). That can facilitate identifying the target by human observer. It should be noted that in the analysis has not been taken into account the obscuration time, the wind speed and direction and did not use full loads. This type of analysis also can provide theoretical values for the minimal concentration of smoke screen to block radiation entirely, which give the necessary mass of smoke composition.

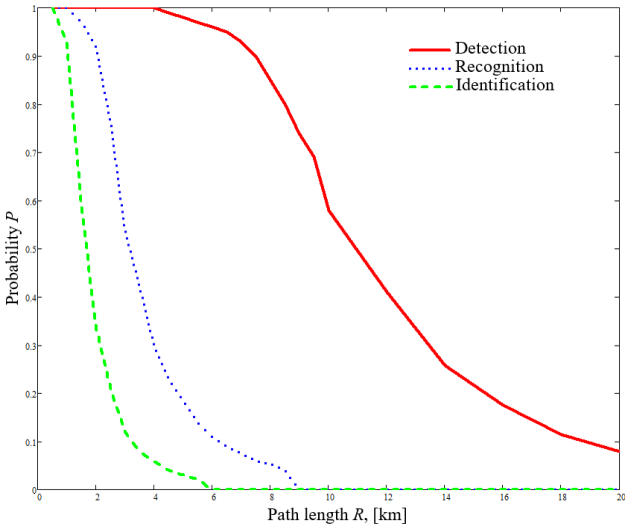

Fig. 7. Discrimination probability in natural atmosphere in the 3-5 µm range

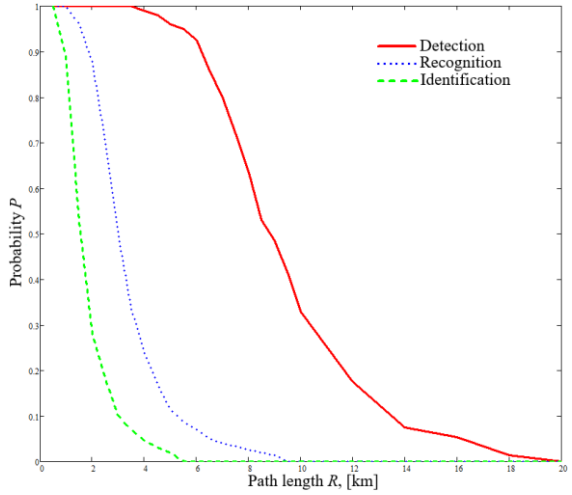

Fig. 8. Discrimination probability in natural atmosphere in the 8-12 μm range

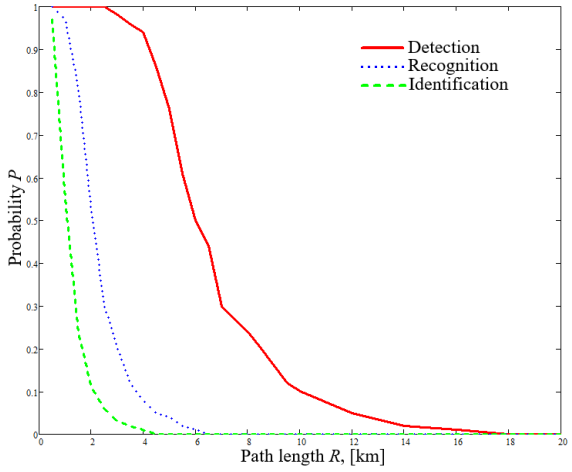

Fig. 9. Discrimination probability in obscurant atmosphere in the 3-5 μm range

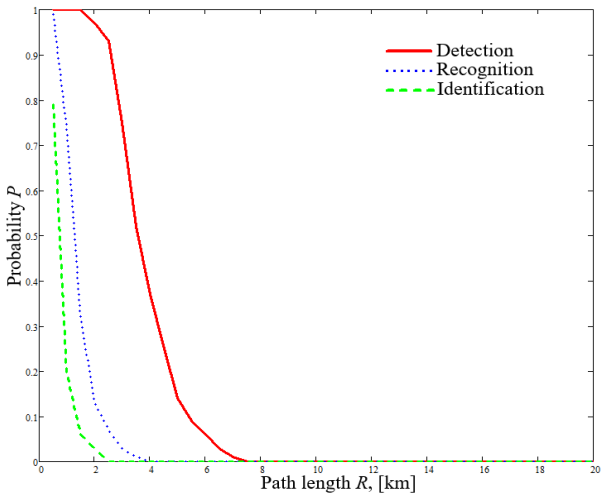

Fig. 10. Discrimination probability in obscurant Atmosphere in the 8-12 μm range

3. Experimental analyses

The experimental part in this work has been divided in two directions of research, one related to understanding the functionality of thermal sensors and the other dedicated to image analysis in Vis and IR spectra by IR obscurants where the human factor has the final decision.

3.1. Experimental part 1

3.1.1. Materials and methods

In order to validate, complete and understand the theoretical information extracted from the literature for thermal systems, an experimental setup has been proposed, where at a distance of 80 cm from the sensor (Fig. 11) a number of objects have been placed in front of a cardboard background, at a temperature of 14.6°C.

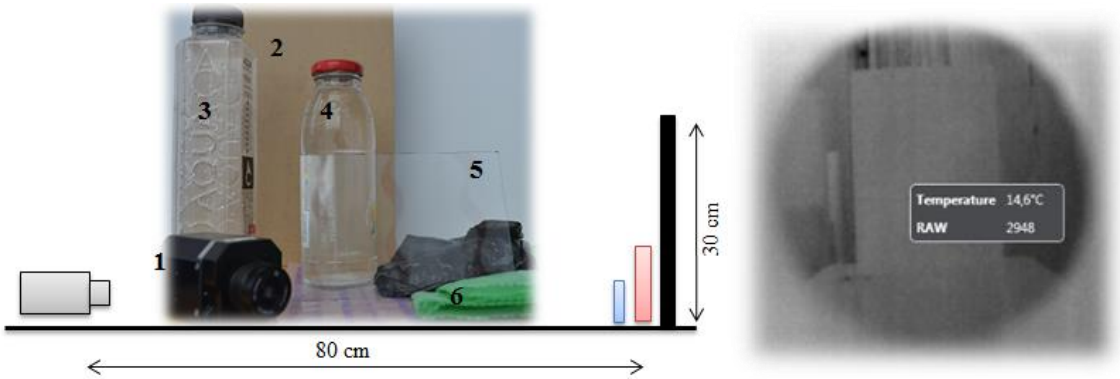

Fig. 11. Test configuration: 1. thermal sensor, 2. background, 3. plastic bottle, 4. glass bottle, 5. glass, 6. plastic foil

A thermal sensor TAU 2 Uncooled Cores 324 has been used for the tests [16], including a digital video display format of 324x256, with uncooled VOx Microbolometer and working in the spectral band 7.5-13.5 μm. The sensor was designed for temperature ranges of -40...+160°C and +160...+550°C. For the image analysis, a dedicated software Core Player was used, allowing saving the temperature histogram over a designated direction (Fig. 12) divided in 12 images.

During the test, the temperature between background and objects and the materials that can influence the propagation of electromagnetic radiations was measured. The test was conducted in laboratory conditions, at 20 °C and 45% relative humidity.

3.1.2. Results and discussion

The first three images from Fig. 12 represent the temperature difference between different objects and background, which influences the thermal image quality. Best image is image 2 (background, empty bottle and hot water bottle – 80°C), where the temperature differences are the highest, as 60°C. Thus, the appearance of objects is based on thermal contrast between the objects and background. In the following two images it can be seen how some objects block human hand emissivity. Here is observed how glass and any plastic material are opaque to the passing of radiation.

It should be noted that although various objects are used at room temperature (empty plastic bottle, empty glass bottle and full plastic bottle), no difference is noted between them. Moreover, from images 5 and 8 can be noted that a plastic foil (0.01 mm thickness) remains transparent also in the thermal spectrum. But by increasing the thickness of the plastic foil (> 0.1mm), a radiation disturbance can be observed (image 9). It is obvious that thermal sensors are affected by variations of water content, as in image 10 (wet plastic bag with raindrop aspect) and image 11 (half a bag of water). The reason why thermal sensors do not use glass materials is shown in image 7.

As expected in thermal vision, the objects images are reflected from shiny surfaces and glass, but do not produce shadows (image 12).

3.2. Experimental part 2

3.2.1. Materials and methods

As discussed in chapter 2, a decrease in the thermal sensors performance is observed when using artificial obscurants, well as the parameters of the atmosphere. But there has not been taken into account the human factor, which is a decisive element in image analysis. In order to complete the theoretical analysis of the observation capacities of thermal sensors, under obscurant conditions, another experimental study has been conducted. The purpose of the experimental study was to observe the generation and dispersion of a smoke screen (visual and thermal scene image) and to analyse these images by human perspective.

Also, during the test, the time in which the smoke screen becomes effective in Vis and IR spectra has been measured. On the one hand, the aim was to compare the performances of visual versus thermal sensors, and to determine the effectiveness of RP smoke screening in Vis and IR spectra.

During the test it was used a modular long range surveillance system „CONDOR-LR", with a thermal camera and a CCD camera for day time vision, developed by PRO OPTICA S.A., Bucharest. Thermal sensors have a digital video display format of 640x512 pixels, cooling detector generation III, optical zoom 20X, detection range 12 km, and recognition range 4.5 km, in the spectral range 3-5 μm. The CCD sensor has HD resolution 1920x1080 pixels, 1/2.8" CMOS detector and optical zoom 30X.

For the obscurant effects it was used a 40 mm smoke grenade (Fig. 13) charged with 160 g RP white smoke composition. The pyrotechnic composition used is a composite mixture based on a strong oxidizer, potassium nitrate (KNO_3, 40-45%), a fuel (RP, 35-50%) and paraffin ($C_{71}H_{148}$, 10-25%) as binder. A generic combustion reaction of this mixture is presented below (17).

In order to confirm in terms of quality the RP-based pyrotechnic composition combustion solid byproducts, the solid residue and the generated aerosols have been analyzed by SEM-EDX and XPS. XPS analysis has been performed using an X-Ray Photoelectron Spectroscopy K-ALPHA (Thermo Scientific). The analysis was performed for each sample three-point, recording for each point general spectra (survey) the binding energy range 0÷1350 eV with an X-ray beam of 400 mm and autofocus area. Energy bands assignment was made by comparing the spectral database with existing literature.

Aerosols generated by RP pyrotechnic composition combustion have been collected on double-sided adhesive carbon discs fixed prior to combustion at 1 and 3 m. Aerosols were analyzed using a VEGA II LMU SEM, resolution 3.5 nm to 30 keV, coupled with a Bruker AXS Microanalysis EDX, Germany, with dedicated software QUANTAX 1.8.2.

The pyrotechnic composition can be loaded in different geometries as shown in Fig. 14, in order to provide a certain burning time and an interval for the generation of the smoke screen.

For these tests, compositions with cylindrical tablet shapes and the following performance characteristics have been employed: combustion heat $Q=2492$ *kcal/kg*, specific volume $V_{sp}=210$ *l/kg*, combustion velocity $V=0.58$ *mm/s* and combustion temperature $T=1027^{o}C$.

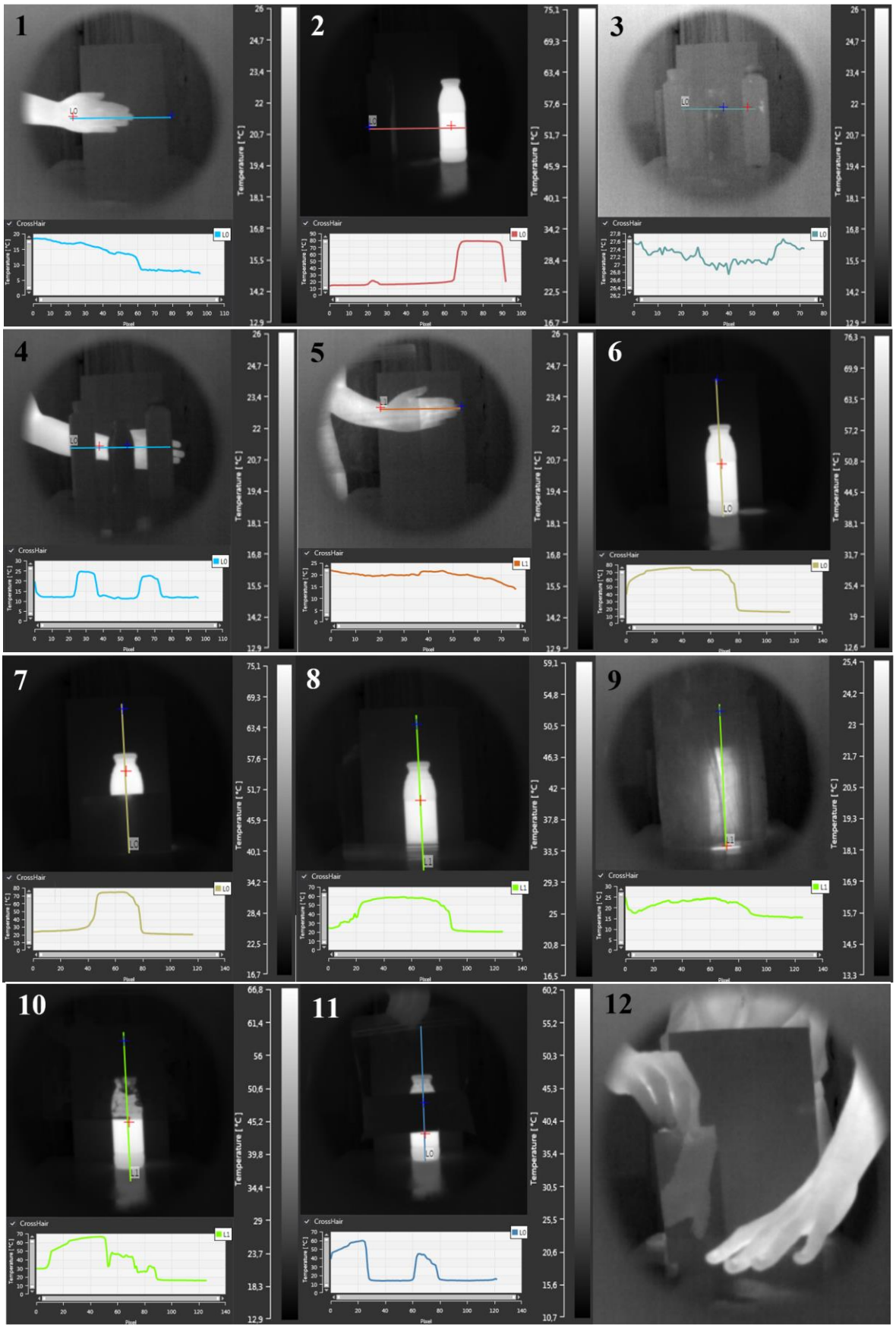

Fig. 12. Thermal temperature histograms.

$$x.KNO_3 + y.P + z.C_{71}H_{148} \rightarrow \alpha.K_2O + \beta.K_3PO_4 + \gamma.P_2O_5 + \delta.P + \varepsilon.C + \theta.H_2 + \mu..H_2O + \sigma.CO_2 + \phi.CO + \varphi N_2 \qquad (17)$$

Fig. 13. 40 mm smoke grenade model

Fig.14. RP smoke composition

For observation purposes, the setup illustrated in Fig. 15, where the smoke grenade is fixed on a frame at 3-6 m away from the target and at 3.5 m height and is initiated by electrical fuse from a safe distance, has been made. The image analysis has been performed for the effect generated by a single 40 mm smoke grenade. The experiment took place at 18°C and 45%average humidity during cloudy conditions.

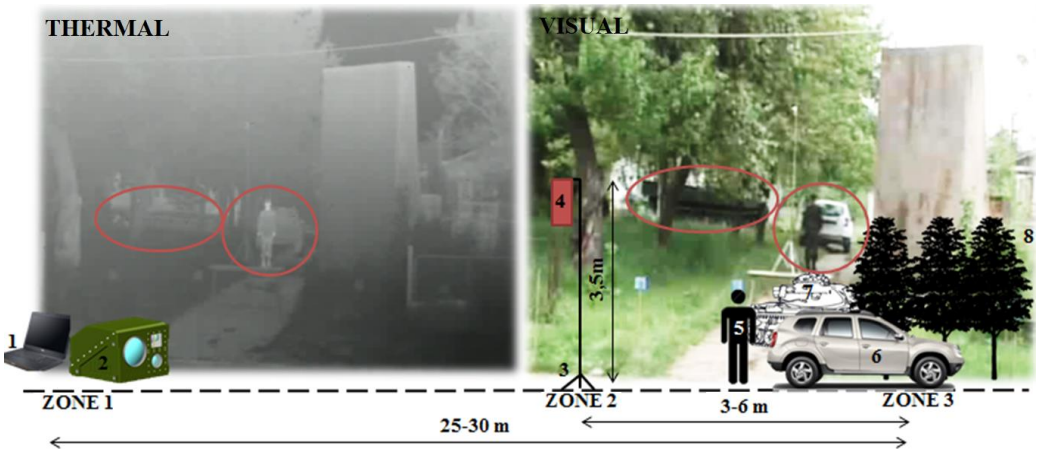

Fig. 15. Testing installation configuration: 1. acquisition and control system, 2. modular optoelectronic system, 3. frame, 4. smoke grenade, 5. human target, 6. civilian vehicle target, 7. military vehicle target, 8. Background.

3.2.2. Results and discussion

Analyzing the results from Fig. 16, it can be seen that the solid byproducts composition consists mainly in K_2O (the existence of O 1s peak at 530.36 eV, highlighting the presence of an oxide) and K_3PO_4, given the existence of P 2p peak at 132.41 eV. Elemental carbon is also present by C 1s at 283.74 eV and possibly a nitrogen-containing organic compound (N 1s at 397.95 eV).

From SEM and EDX analyses, it can be seen that the solid particles of the aerosol generated by the pyrotechnic composition are homogeneous both in terms of the composition and dimensions. The obtained particles are in the nanometer range and gather in flocks, thus providing a good masking (Fig. 17 and Fig. 18).

EDX analysis and linear profile obtained (Fig. 18) confirm the results obtained by XPS, that the major product contains K and P, which leads to the existence of K_3PO_4 as main solid byproduct.

Further, 10 smoke grenades were fired, generating similar obscuring effects. In order to have a comparative analysis, a strip of images was achieved (Fig. 19), where relevant details can be noted regarding target observation. The images were sampled by editing the movies recorded during the test. Since the human observer is the decisive factor, the images were analysed only visually.

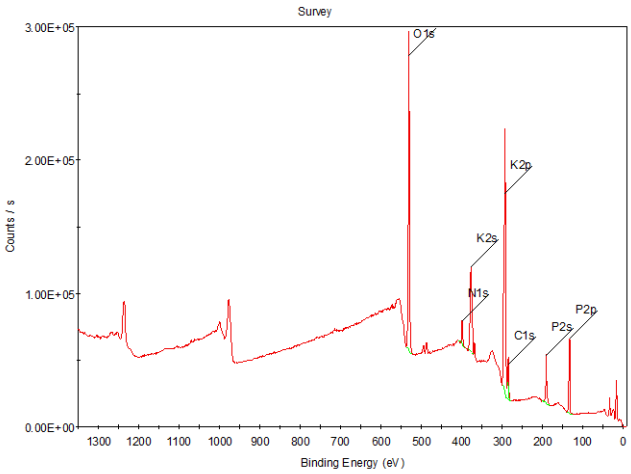

Fig. 16. XPS analysis of aerosols

For a single charge, the concealment time in IR region was 2.5 s and approximately 16 s in the Vis region. The moment of burst and screen generation and dispersion can

be observed in images 2-4, with similar aspects in Vis and IR spectra. The screen becomes effective in Vis starting with images 5-6 (after approx. 1 second) and in IR starting with image 4 (after approx. 0.5 seconds).

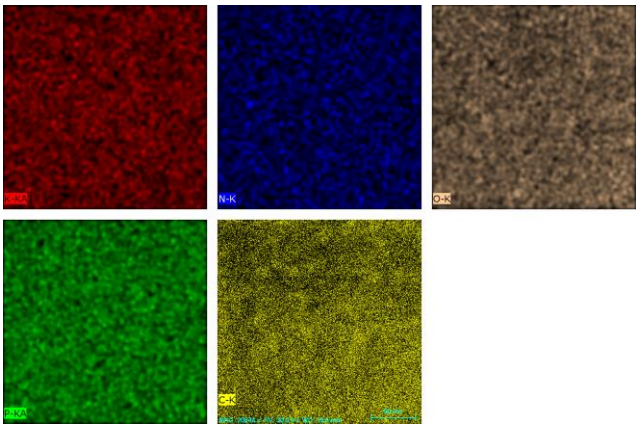

Fig. 17. Photomicrographs with elemental distribution in the aerosol

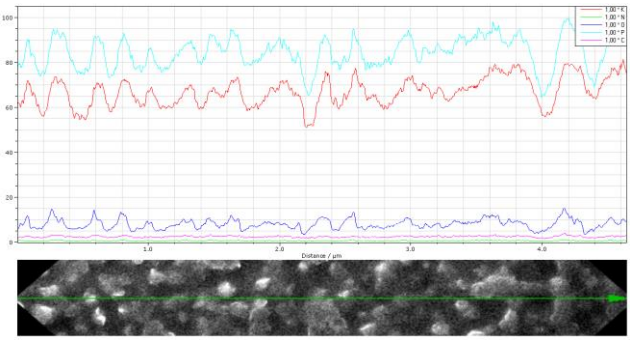

Fig. 18. EDX linear profile with elemental distribution in the aerosol

Starting with image 7 (after approx. 3 seconds) the target detection in IR becomes possible and in image 8 the target can be recognised and identified from other background objects In the Vis spectrum, the target is still concealed after 16 s. The initial obscuration of the vehicle and the human body against thermal systems is caused by the radiant heat of pyrotechnic combustion and ends with reaction products cooling. It is observed the fact that the smoke screen causes a small attenuation of electromagnetic radiation at 30-m distances in the IR spectrum and blocks entirely the radiation in Vis spectrum.

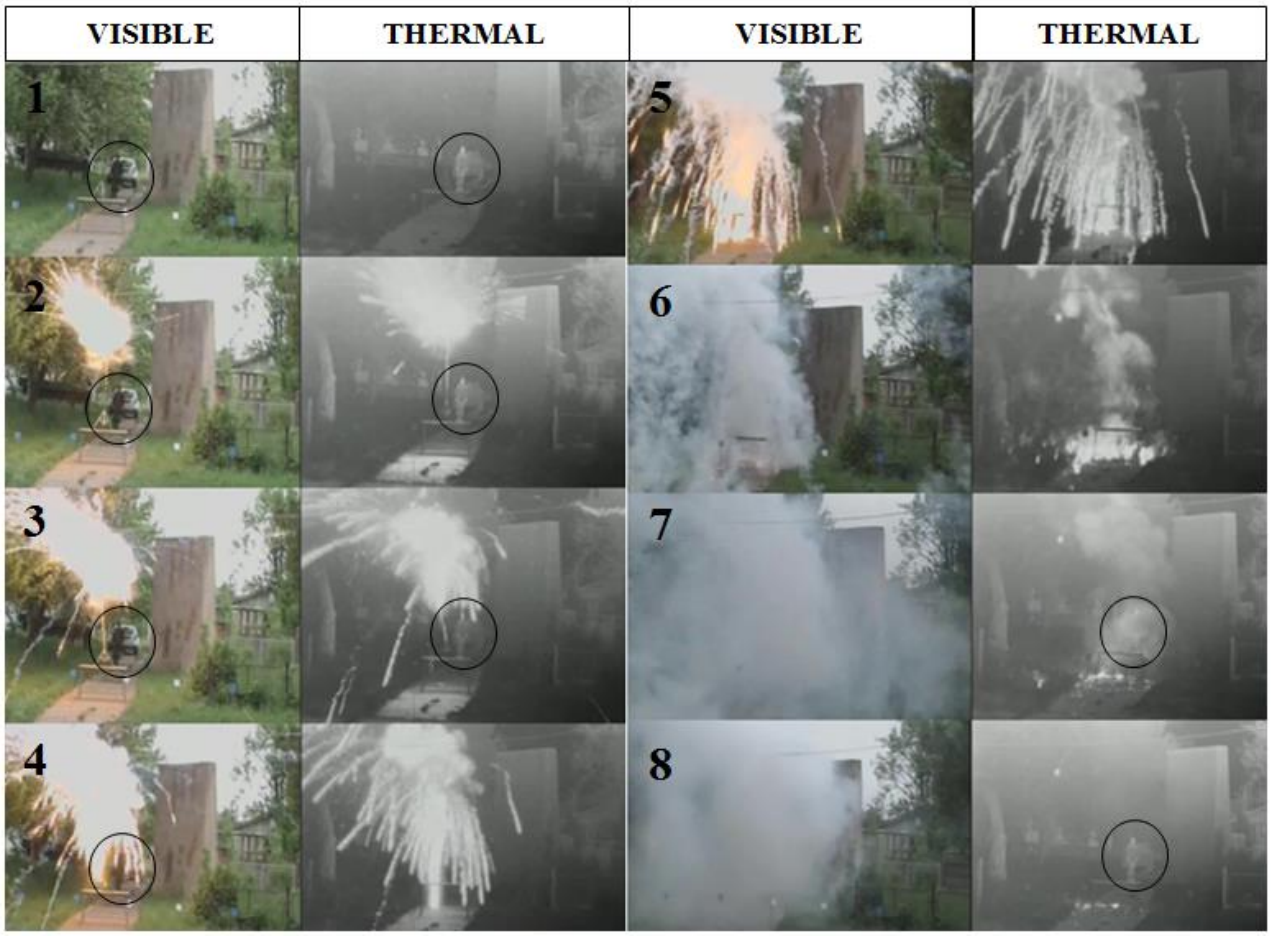

Fig. 19. Smoke screen dispersion in Vis and IR spectra

4. Conclusions

In the field of night vision systems, thermal sensors are superior to any other existing optoelectronic systems. IR sensors present high performances regarding target observation in harsh conditions and an important efficiency against military obscurants. Using a Johnson model, in a first theoretical approach, this study showed how atmospheric conditions and artificial obscurants influence the target discrimination probability for a thermal system. It has been concluded that for thermal systems operating in the spectral region 8-12 μm, the target signature is more affected by the atmospheric attenuation.

By experimental setups, the performances and limitations of the thermal sensors operating in the IR spectrum were emphasized.

The performances of Vis and IR sensors in the presence of artificial obscurants have been investigated comparatively and the conclusion is that, although concealment is possible, the obscuring time in IR is relatively short and requires larger pyrotechnic charges and well thought battle tactics.

References

[1] J. A. Conkling, C. Mocella, Chemistry of Pyrotechnics: Basic Principles and Theory, Second Edition, CRC Press (2010).
[2] R. Ramos, H. Boschi-Filho, Physica A: Statistical Mechanics and its Applications 393 (2014).
[3] Z. Zhou, M. Dong, X. Xie, Z. Gao, Applied Optics **55**, 23 (2016).
[4] K. Smit, A. Lee, M. Burridge, Infrared and Visual Smoke Countermeasures for Army, DSTO External Publication (2008).
[5] C. Song, J. Gao, X. Zhang, J. Optoelectron. Adv. M. **17**(1-2), 7 (2015).
[6] H. Li, X. Chen, Optoelectron. Adv. Mat. **9**(7-8), 907 (2015).
[7] B. Feng, J. Ni, Z. Wu, Optoelectron. Adv. Mat. **10**(1-2), 40 (2016).
[8] Sagem Defense Securite, Groupe Safran, MOST The Optronic Mast For Land Surveillance.
[9] Sagem Defense Securite, Groupe Safran, Paseo Modular Advanced Stabilized Sight.
[10] T. Zecheru, A. Lungu, P.-Z. Iordache, T. Rotariu, Combustion, Explosion and Shock Waves **49**, 2 (2013).
[11] FM 3-50, Smoke Operations, Headquarters Department of the Ramy, Washington, DC (1996).
[12] C. Lăzăroaie, S. Eşanu, C. Său, R. Petre, P. Z. Iordache, G. Staikos, T. Rotariu, T. Zecheru, Journal of Thermal Analysis and Calorimetry **115**, 2 (2014).
[13] T.V. Ţigănescu, R. Ştefănoiu, T. Rotariu, M. Lupoae, Revista de Chimie **58**(7), 688 (2007).
[14] Military Handbook, Quantitative description of obscuration factors for electro-optical and millimetre wave systems, Department of Defence, METRIC (1986).
[15] A. Wetmore, S.D. Ayres, COMBIC, Combined Obscuration Model for Battlefield Induced Contaminants, Army Research Laboratory (2000).
[16] http://www.flir.com/cores/display/?id=54717.

*Corresponding author: traian.rotariu@gmail.com